Comparison of classical and ab initio simulations of hydronium and aqueous proton transfer Θ

Manuela Maurer 💿 ; Themis Lazaridis 🗷 👵



J. Chem. Phys. 159, 134506 (2023) https://doi.org/10.1063/5.0166596





Citation

CrossMark

Articles You May Be Interested In

On integrable potential perturbations of the billiard system within an ellipsoid

J. Math. Phys. (June 1997)

500 kHz or 8.5 GHz? And all the ranges in between.

Lock-in Amplifiers for your periodic signal measurement









Comparison of classical and ab initio simulations of hydronium and aqueous proton transfer

Cite as: J. Chem. Phys. 159, 134506 (2023); doi: 10.1063/5.0166596

Submitted: 6 July 2023 • Accepted: 25 September 2023 •

Published Online: 5 October 2023









Manuela Maurer¹ and Themis Lazaridis^{1,2,a)}



AFFILIATIONS

- Department of Chemistry, City College of New York/CUNY, 160 Convent Ave., New York, New York 10031, USA
- ²Graduate Programs in Chemistry, Biochemistry, and Physics, The Graduate Center, City University of New York, 365 Fifth Ave., New York, New York 10016, USA

ABSTRACT

Proton transport in aqueous systems occurs by making and breaking covalent bonds, a process that classical force fields cannot reproduce. Various attempts have been made to remedy this deficiency, by valence bond theory or instantaneous proton transfers, but the ability of such methods to provide a realistic picture of this fundamental process has not been fully evaluated. Here we compare an ab initio molecular dynamics (AIMD) simulation of an excess proton in water to a simulation of a classical H₃O⁺ in TIP3P water. The energy gap upon instantaneous proton transfer from H₃O⁺ to an acceptor water molecule is much higher in the classical simulation than in the AIMD configurations evaluated with the same classical potential. The origins of this discrepancy are identified by comparing the solvent structures around the excess proton in the two systems. One major structural difference is in the tilt angle of the water molecules that accept an hydrogen bond from H₃O⁺. The lack of lone pairs in TIP3P produces a tilt angle that is too large and generates an unfavorable geometry after instantaneous proton transfer. This problem can be alleviated by the use of TIP5P, which gives a tilt angle much closer to the AIMD result. Another important factor that raises the energy gap is the different optimal distance in water-water vs H₃O⁺-water H-bonds. In AIMD the acceptor is gradually polarized and takes a hydronium-like configuration even before proton transfer actually happens. Ways to remedy some of these problems in classical simulations are discussed.

Published under an exclusive license by AIP Publishing. https://doi.org/10.1063/5.0166596

I. INTRODUCTION

The products of water self-dissociation are present at low concentrations but have dramatic influence on chemical and biochemical processes. Introductory textbooks show the excess proton added to a water molecule to form the hydronium cation (H₃O⁺). Hydronium H-bonds strongly to three H₂O molecules, forming the C3-symmetric Eigen cation [H₉O₄]⁺. Alternatively, the proton can be shared equally between two water molecules, forming the C2-symmetric Zundel cation $[H_5O_2]^+$. Whether Eigen or Zundel is the dominant form in protonated water has been debated for a good while.¹⁻³ The picture that emerges from most theoretical calculations is that the excess proton forms an Eigen cation that is distorted from C3 symmetry because at any given time the H₃O⁺ associates more closely with one of its three hydrogen bonded partners (the

Proton/hydroxide transport plays important roles in chemistry and biochemistry. Proton diffusion in water takes place by hopping of protons between hydrogen bonded water molecules (the Grotthuss mechanism, or structural diffusion). This is why H₃O⁺ has a diffusion coefficient of 0.93 Å² ps⁻¹, while the water self-diffusion coefficient is only 0.23 $\text{Å}^2 \text{ ps}^{-1}$. The passing of a proton from one water molecule to the next takes about 0.5 ps. The proton has to move only ≤ 1 Å while electronic charge transfer changes the two involved bonds from covalent to hydrogen bond and vice versa. The proton transfer (PT) process is thus commonly described as a transition from one distorted Eigen complex to another via a Zundel intermediate,4 with the interconversion between Eigen and Zundel taking less than 100 fs.9

Because proton diffusion involves bond making and breaking, the natural approach to study this process is quantum mechanics. Significant insights have been obtained by ab initio molecular dynamics (AIMD) simulations over the past two decades. 10-13 However, the large computational expense severely limits the timescale and the size of the systems studied; most proton transport processes in biochemical systems are beyond the reach of AIMD methods.

^{a)}Author to whom correspondence should be addressed: tlazaridis@ccny.cuny.edu. Tel.: (212) 650-8364.

This led to the development of more approximate empirical or semiempirical methods. Most extensively employed is the Multistate Empirical Valence Bond method 14,15 where the state of the system is a hybrid of classical states with the proton at a different location. Other methods include Q-HOP, 16 λ -dynamics, 17 ReaxFF, 18 and various empirical schemes. 19,20

Our lab recently proposed an algorithm called mobile hydrogen (MOBHY). In the current implementation of MOBHY into the CHARMM program 22 a proton hop is an instantaneous event. With all surrounding atoms fixed, the difference in potential energy upon transferring the proton (ΔE_{hop}) is calculated. A Metropolis-like criterion is used to determine if the exchange is accepted or rejected. The solvation shell can only adapt after the hop is accepted and regular MD simulation resumes. ΔE_{hop} is typically very high due to the sudden change. Experimentally however, the energy barrier for water-water proton transfer is very low, because the solvation shell molecules adapt gradually already during migration of the charge defect. One may justifiably wonder to what extent these classical trajectories resemble the AIMD trajectories and how the realism of the classical trajectories could be improved.

To that end, we compare here an *ab initio* molecular dynamics (AIMD) simulation trajectory of an excess proton in water²³ to classical MD simulation trajectories of hydronium in water. We first calculate the instantaneous proton hopping energy gap in both systems and then examine differences in structure that can account for the observed differences in the energy gap. Finally, we discuss ways that these differences can be reduced and the realism of classical MD improved. This work focuses on solvation structure and its effect on single proton hopping energetics. Dynamic effects, such as rattling^{23–25} or burst and rest behavior,^{26,27} require a different type of analysis which is left for future work.

II. METHODS

An *ab initio* trajectory of an excess proton in water²³ was generously provided by Prof. Mark Tuckerman. The 30.6-ps

microcanonical simulation used DFT-based Car-Parrinello MD with B-LYP functionals and DVR basis functions on 32 water molecules and one excess proton in a cubic periodic box of edge length 9.87 Å. No dispersion corrections were included in that study. Later work found significant effects of such corrections on OH⁻ solvation but confirmed the basic picture of PT by H₃O⁺. ^{13,28} For our analysis, we extracted configurations from the trajectory at a 2 fs interval, leading to 15 300 coordinate frames. Hydrogens were assigned to the closest O and the O with three assigned H was identified as the H₃O⁺. To make energy calculations comparable to CHARMM and to detect hydrogen bonds into the second solvation shell, we added copies of the system around the central simulation box (one layer of periodic images). In these copies, the excess proton was removed. This resulted in a cubic box of 29.6 Å side length with 863 solvent molecules and one H₃O⁺ ion. The ab initio simulation box was always centered at the hydronium O. We used a geometric criterion (covalent OH bond length > 1.15 Å) to define AIMD frames involved in PT and distinguish them from non-transfer frames (see Fig. S1 in supplementary material for justification).

All classical simulations used 982 solvent molecules and one H₃O⁺ ion, in a cubic box of 31.1 Å initial edge length. The simulations were equilibrated for at least 10 ps. Production was run for 1 ns using constant temperature and pressure with a Hoover thermostat (300 K) and a Langevin barostat (1.0 bar). A 2-fs time step was used for simulations with SHAKE and 1-fs for freely vibrating simulations. Trajectories were written out such that each contained 25 000 frames, resulting in about 50 000-70 000 hop attempts per classical system. We employed Particle Mesh Ewald for the long range electrostatics and the TIP3P water model (CHARMM version with LJ-potential on H). For the excess proton we chose the Sagnella-Voth (svH3O) model of H₃O^{+,29} which is similar in spirit to the TIP3P water model. Another model with increased atomic partial charges aimed to reproduce the experimental solvation free energy in TIP3P²¹ is referred to as the polarized hydronium model (pH3O). For reasons that will become evident below, we also performed and

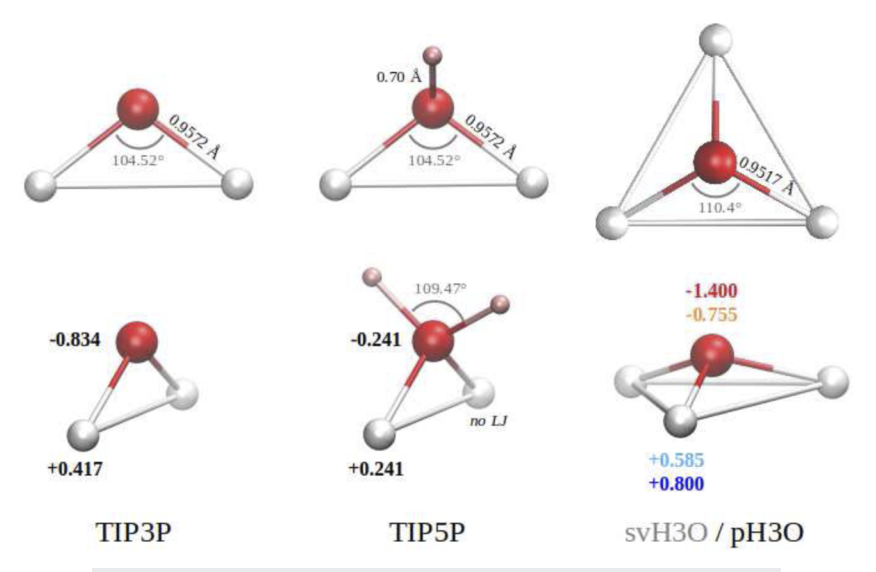


FIG. 1. Molecular models used in this work. Charges in e and bold font, angles in gray.

analyzed simulations in TIP5P solvent.³⁰ An overview of the models used in this work is given in Fig. 1.

The hopping energy gap (ΔE_{hop}) was calculated with either the MOBHY module of CHARMM (only for TIP3P solvent) or more generally with a "coordinate swapping" CHARMM script. We used this script to analyze all trajectories. To start, we added the missing TIP5P lone pair particles to AIMD's atomic coordinates before initial energy evaluation. Our script then iterated through the three closest acceptor molecules, successively exchanged the coordinates of each H₃O⁺ donor and H₂O acceptor pair, and optionally also adjusted the hydrogen atoms to an idealized position, similar to the way MOBHY uses geometric rules to place the new hydrogen after a protonation status exchange. In all protocols, any lone pair particles are regenerated according to the new atomic positions before a final energy evaluation.

We limit the selection of potential proton acceptors to water molecules within the first solvation shell, i.e. to solvent molecules that have their oxygen within 2.9 Å (classical TIP3P, AIMD) or 2.7 Å (classical TIP5P) of the hydronium oxygen. We defined this cutoff according to the respective radial distribution functions (see Results). For the analysis of water - water H-bonds that the acceptor molecules make, we analogously use 3.25 Å. We limited the D-H···A hydrogen bond angle to 40° off-linearity (parameter cuthba 40 in CHARMM's hbond facility). In the classical simulations we discarded all configurations where the H₃O⁺ is within 3 Å of the box boundary either before or after the hop.

Solvation free energy calculations were conducted with the PERT module of CHARMM by converting the single H₃O⁺ into either TIP3P or TIP5P and adding the solvation free energy of a water molecule. Ten evenly spaced perturbation windows were run for 10 ps each, using a 1-fs time step, and the first 2 ps of each window were discarded.

III. RESULTS

A. Energy gap and its decomposition

ΔE_{hop} is the difference in potential energy (energy gap) upon instant PT. We first evaluate ab initio trajectory configurations with

TABLE I. ΔE_{hop} in AIMD configurations evaluated with classical potentials (kcal/mol). In the upper part of the table the covalent bond of H3 (the transferred proton) is adjusted to the same length after a hop as it had before a hop. In the lower part of the table an ideal hydronium configuration is imposed before and after the hop. Error bars are standard

	In TIP3		In TIP5	
	svH3O	рН3О	svH3O	рН3О
With vibrating b	onds, minimal H3 co	ordinate adjustment		
All configurations	15.2 ± 10.5	15.1 ± 12.6	15.5 ± 10.4	18.1 ± 13.3
All covalent bonds < 1.15 Å (36 330 hop attempts)	15.3 ± 9.9	14.8 ± 12.0	16.3 ± 9.8	18.2 ± 12.6
Along a covalent bond > 1.15 Å (3094 hop attempts)	4.2 ± 8.6	4.0 ± 11.3	4.2 ± 8.8	4.4 ± 11.9
Mid-PT configurations (302 hop attempts)	-0.1 ± 8.0	-0.2 ± 11.0	-0.3 ± 8.5	-0.4 ± 11.4
With SHA	AKE before + after, all	H's idealized		
All configurations	13.4 ± 8.5	13.3 ± 10.3	14.9 ± 9.1	16.4 ± 11.6
All covalent bonds < 1.15 Å (36 330 hop attempts)	13.9 ± 8.0	13.6 ± 9.9	15.5 ± 8.6	16.8 ± 11.1
Along a covalent bond > 1.15 Å (3094 hop attempts)	4.5 ± 8.1	4.9 ± 9.7	4.8 ± 8.6	5.5 ± 11.1
Mid-PT configurations (302 hop attempts)	1.4 ± 7.4	1.9 ± 9.2	0.9 ± 7.9	1.4 ± 10.5

TABLE II. ΔE_{hop} and its decomposition in classical and AIMD trajectories (kcal/mol). Constant bond lengths enforced in all trajectories at all times. Error bars are standard deviations.

		ΔE_{hop}	$\Delta E_{don ext{-}acc}$	$\Delta E_{don\text{-}1st}$	$\Delta E_{don\text{-}env}$	$\Delta E_{acc\text{-env}}$	ΔE_{rem}
			Class	sical trajectories			
svH3O	svH3O	38.3 ± 8.4	10.1 ± 4.7	22.7 ± 12.8	-1.0 ± 9.2	-4.0 ± 3.5	10.5 ± 15.5
TIP3P	рН3О	47.6 ± 10.0	15.5 ± 5.7	27.8 ± 14.8	-0.4 ± 10.4	-5.5 ± 3.6	10.1 ± 17.5
TIP5P	svH3O	31.1 ± 7.0	1.3 ± 2.4	33.8 ± 13.0	-9.4 ± 11.1	-1.1 ± 3.6	6.5 ± 17.3
1117517	pH3O	37.6 ± 7.6	1.4 ± 2.4	44.1 ± 15.4	-12.8 ± 12.8	-0.1 ± 3.9	4.9 ± 20.2
		AIMD tra	ectory evaluated w	rith classical potenti	als (all cov < 1.15 Å)		
TIDAD	svH3O	13.9 ± 8.0	1.6 ± 5.2	7.2 ± 11.6	-1.3 ± 6.8	4.6 ± 4.6	1.8 ± 13.2
TIP3P	рН3О	13.6 ± 9.9	2.4 ± 6.7	7.6 ± 14.3	-2.5 ± 7.5	4.6 ± 4.6	1.4 ± 15.5
TIDED	svH3O	15.5 ± 8.6	1.4 ± 5.3	11.8 ± 13.4	-1.6 ± 7.3	2.4 ± 4.1	1.4 ± 14.9
TIP5P	рН3О	16.8 ± 11.1	2.2 ± 6.8	13.8 ± 16.8	-2.7 ± 8.2	2.4 ± 4.1	1.0 ± 17.9

classical potentials in Table I (Fig. S2 in supplementary material shows the complete distributions). The energy gaps are similar regardless of the classical potential used to evaluate them. The configurations with a hydronium O–H covalent bond longer than 1.15 Å (signifying a system en route to proton transfer) have substantially lower energy gaps, as expected. Those in the middle of a PT event are even lower. For the remainder of this text, we will by default only include non-hopping AIMD frames into our analyses where all of hydronium's covalent bonds are shorter than 1.15 Å. The energy values do not change much if one idealizes the hydronium structure before and after the hop, and they are substantially lower than those obtained from classical MD in Table II. Regardless of the hopping protocol and classical potential used, AIMD's ΔE_{hop} average remains almost the same, and a sizeable fraction of configurations gives a negative ΔE_{hop} .

The same calculation on classical configurations shows much higher energy gaps (Table II and Fig. S2). To determine the origin of the large difference in ΔE_{hop} between classical and AIMD configurations we decomposed it into several contributions: (a) the donor H_3O^+ -proton acceptor interaction, (b) the interaction of H_3O^+ with the 1st solvation shell waters other than the proton acceptor, (c) the interaction of H_3O^+ with all molecules beyond its 1st shell, (d) the interaction of the proton acceptor with all molecules except H_3O^+ , (e) the remainder, which includes long range electrostatic effects (Ewald). That is,

$$\begin{split} \Delta E_{hop} &= \Delta E_{don-acc} + \Delta E_{don-1st} + \Delta E_{don-env} \\ &+ \Delta E_{acc-env} + \Delta E_{rem} \end{split} \tag{1}$$

The results are also shown in Table II. Two terms are striking: first, the donor-acceptor interaction makes a large contribution in TIP3P, but not in TIP5P. This term is small and similar to TIP5P in the AIMD configurations. Second, the donor-1st shell contribution in both classical systems is much larger than in the AIMD configurations. This means that the main contribution to the instant PT energy gap comes from those close molecular contacts in the 1st solvation shell that are exchanged and unequilibrated after the hop. The structural causes of these differences are investigated in Sec. III B.

B. Structural comparison

1. Radial distribution function (RDF)

Figure 2 shows the $O^* \cdots O$ RDF in the different systems (O^* is hydronium's oxygen). We only calculate the RDF up to a radius of 5 Å for the AIMD system (grey) because the original cubic simulation box is only ~10 Å long. For comparison with experimental data, see our previous work.²¹ Several important differences are seen between the classical and quantum trajectories. The 1st peak is higher in the classical trajectories and in some cases too far (svH3O in TIP3P) or too close (pH3O in TIP5P). pH3O in TIP3P and svH3O in TIP5P show a 1st solvation shell peak at about the right distance. Striking is also the lack of 2nd solvation shell peak in TIP3P. It is a known structural deficiency of the TIP3P water model that the pure water O···O RDF lacks a second peak,³¹ and this seems to carry over to H₃O⁺ solvation too (our RDFs of pure H₂O in the different systems can be found in Fig. S3 in supplementary material). TIP5P does a much better job reproducing the 2nd solvation shell peak.

We also calculated the solvation free energies ΔG_{solv} for the four classical models' combinations. For the svH3O model, we calculated a solvation free energy of -84.6 ± 0.7 kcal/mol in TIP3P and -108.6 ± 0.3 kcal/mol in TIP5P. For the pH3O model, we calculated -97.2 ± 0.3 kcal/mol in TIP3P and -129.6 ± 0.8 kcal/mol in TIP5P. The experimental value is -95.6 to -101.6 kcal/mol. 32,33 Thus, svH3O in TIP5P and pH3O in TIP3P give results closer to experiment, in line with the more accurate position of the 1st RDF peaks.

All four combinations of classical models show significant density near the 1st minimum of the AIMD RDF around 2.9 Å. TIP5P actually features a low peak right at 2.9 Å. We term this region between the end of the 1st and the beginning of the 2nd solvation shell the "1.5th solvation shell" and investigate it in detail in Figs S4 and S5 in supplementary material. The region is basically populated by three kinds of molecules (refer to Fig. 3): (a) directly above the $\rm H_3O^+$, donating or almost donating an H-bond to it; (b) slightly above the three H-bonded acceptors, in the interstices between them, with a range of orientations; (c) directly below the $\rm H_3O^+$, with hydrogens pointing straight away. Most molecules reside in the hemisphere above $\rm H_3O^+$, and at least 93% of them are not

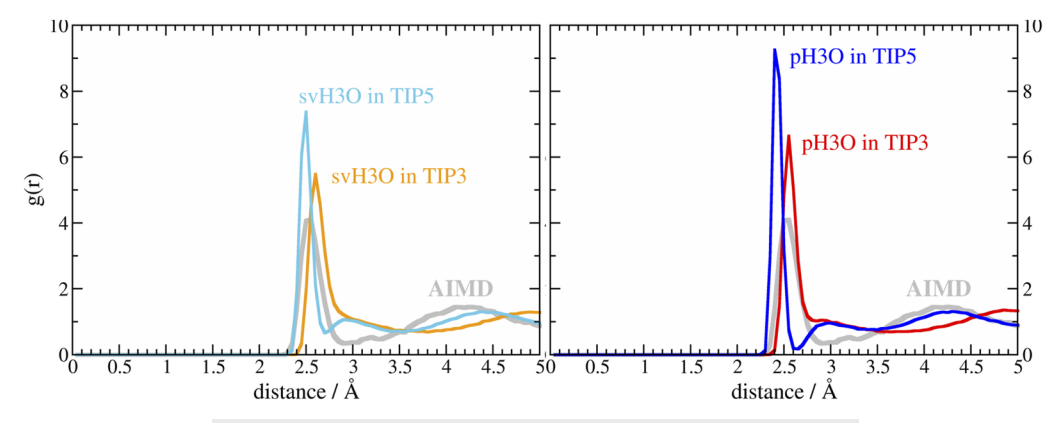


FIG. 2. Radial distribution functions of solvent oxygen around hydronium oxygen.

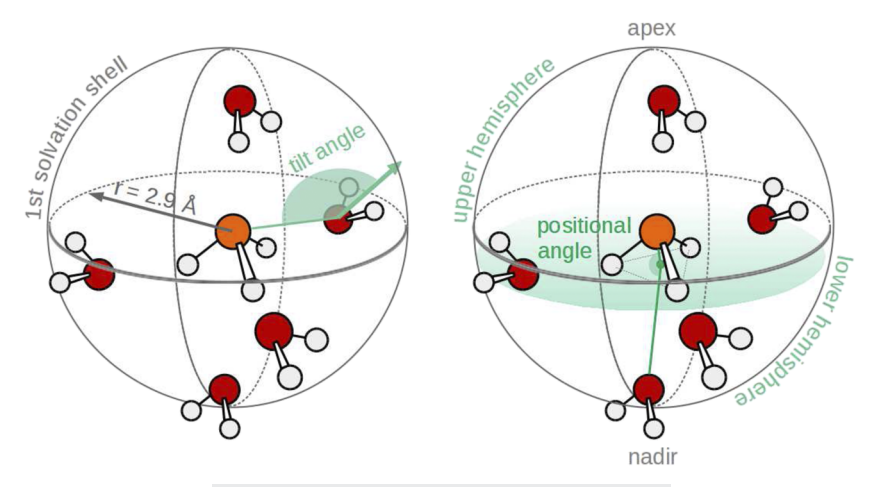


FIG. 3. Tilt and positional angle in the 1st solvation shell.

H-bonded to the donor-acceptor complex in any way, according to our definition, both in TIP3P and TIP5P. There are comparatively more molecules right above and especially right below $\rm H_3O^+$ in TIP5P than in TIP3P. This position is probably favored due to the three TIP5P acceptor molecule's H-bonds extending into the solvent at a steeper angle than in TIP3P. The population shift from fluctuating interstitial to more permanently occupied apex and nadir positions seems to cause the local difference between the TIP3P and TIP5P RDFs, respectively.

Due to their RDF and ΔG_{solv} , from here on we will focus only on pH3O in TIP3P and svH3O in TIP5P. All calculations were also conducted with svH3O in TIP3P and pH3O in TIP5P (results not shown). The calculated RDFs are used to define the 1st solvation shell for the analyses that follow as an oxygen-oxygen distance of 2.9 Å for AIMD and TIP3P, and 2.7 Å for TIP5P. We also use waterwater O···O distance to define the cutoff for purely water-water H-bonds as 3.25 Å, based on Fig. S3.

2. Tilt and positional angles, before the hop

We now investigate the structure of the 1st solvation shell. The D-H···A H-bond angle only gives information on donor orientation. Information on an acceptor's orientation is given by its tilt angle, defined as the angle between its dipole moment vector and the O*O vector (Fig. 3). Visual examination of the trajectories showed that TIP3P acceptors adopted a tilt angle close to 180°, whereas AIMD waters had a tilt angle closer to 135°, pointing a lone pair to the hydronium. Isolated hydronium with TIP3P or TIP4P in the gas phase produced a similar orientation. Only TIP5P with its explicit lone pairs was able to reproduce the tilting observed in AIMD. That was the motivation for extending our studies to TIP5P.

We also define a positional angle (Fig. 3) to describe a molecule's placement in the 1st solvation shell relative to H_3O^+ . We define it as the angle formed by the hydronium oxygen, the center of geometry of its three hydrogens, and the acceptor water oxygen. Hydronium's hydrogens reside at exactly 90° when the molecular geometry is ideal. A water molecule above the apex is at 0° and below

the pyramid is at 180° . The positional angle informs us on where H_3O^+ is facing relative to the acceptor.

The large panels of Fig. 4 (left) show a scatter plot of the tilt and positional angles of 1st solvation shell molecules. Their respective marginal probability distributions are shown in the small panels attached to the left or below. TIP3P (red) and especially AIMD (gray) molecules show a wide range of tilt angles, while TIP5P (cyan) molecules, once H-bonded, show a more limited range of tilt angles. TIP5P's average tilt angle matches AIMD well at ~130° but the average tilt angle of H-bonded TIP3P acceptors is too large, at ~160°, with H1 and H2 pointing more or less directly away from the donor. The positional angles of both models match the AIMD result quite well.

3. Tilt and positional angles after the hop

Upon PT, the H3 of the donor is added to the acceptor at a position compatible with hydronium's idealized pyramidal geometry. The tilt and positional angles after a hop are shown in the right panels of Fig. 4. The left and right side are very similar for TIP5P and AIMD. The positions of the gray main peaks remain virtually the same. The only difference between pre- and post-hop situation is that a small additional peak appears at $\sim\!50^\circ$ tilt angle and right above the H_3O^+ , where a molecule from the 2nd solvation shell has donated an H-bond to an acceptor; this bond is now donated to the new H_3O^+ post-hop. For classical TIP5P, the same small population appears in dark blue in Fig. 4, where the color indicates an unfavorable $H_3O^+\cdots H_2O$ interaction energy.

In the classical TIP3P trajectory however, pre- and post-hop situation differ substantially. A new peak appears at ${\sim}50^{\circ}$ in the positional angle distribution, corresponding to the water molecule the proton just came from. That is a bit above the hydrogen plane, and off from either a proper accepting or donating position. The dark red and magenta colors in Fig. 4 indicate an (unfavorable) interaction energy between $\rm H_3O^+$ and a TIP3P of higher than -10 and higher than 0 kcal/mol, respectively. This population of water molecules where the proton just came from shows predominantly these colors.

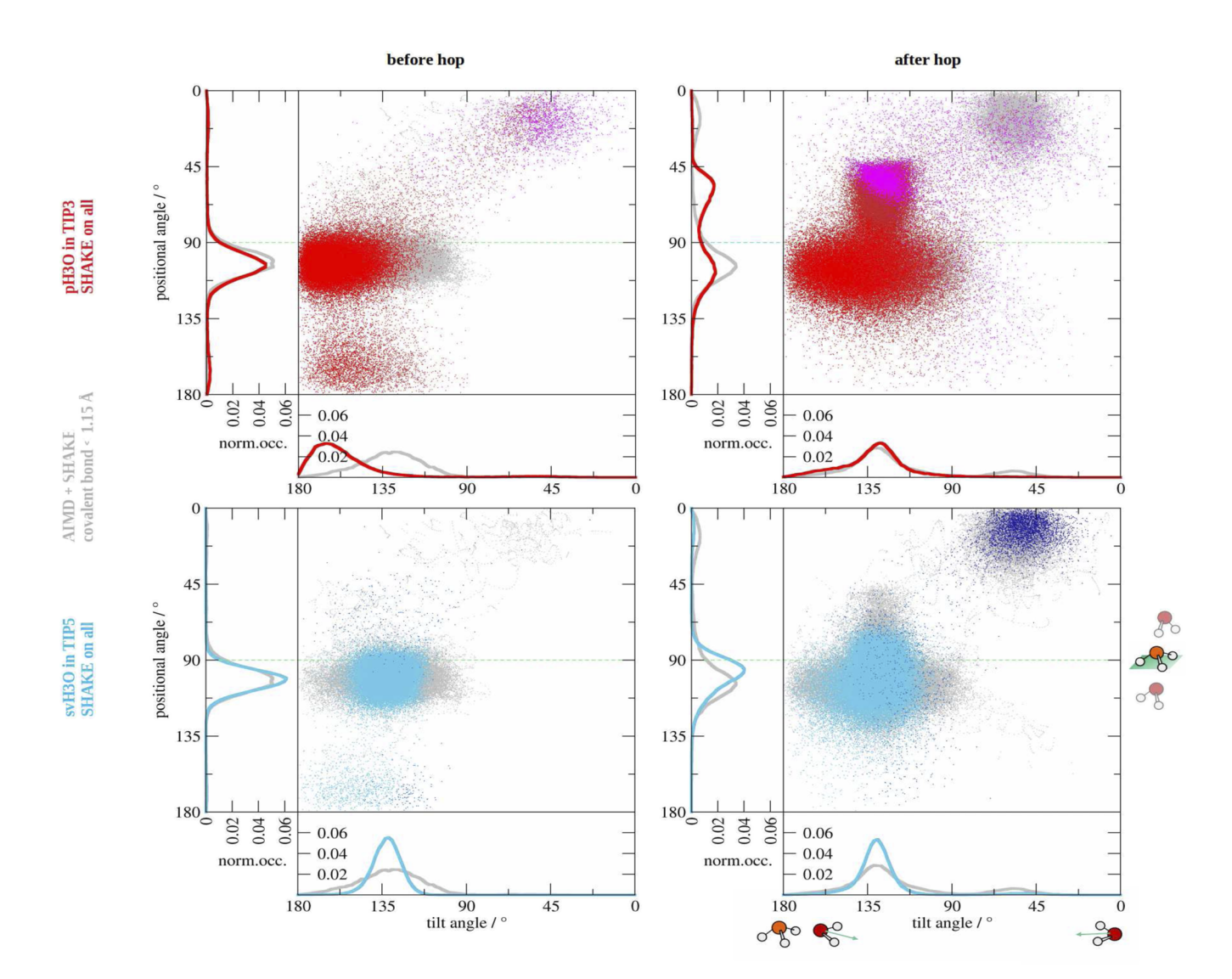


FIG. 4. The structure of the 1st solvation shell, as shown through tilt angles and positions. Classical trajectories were created with SHAKE, and SHAKE was applied to AIMD hydrogen coordinates for comparability. Both donor and acceptor geometries were fully idealized after the hop. Unfavorable subpopulations are colored dark red and magenta for TIP3P, and medium and dark blue for TIP5P; these denote interaction energies of that water molecule with H₃O⁺ higher than -10 and 0 kcal mol⁻¹, respectively. Visualizations of the hydrogen plane and tilt angle are depicted in green. The complete graph collection for all investigated systems can be found in Fig. S6 in the supplementary material.

All this happens because the transferred H3 proton has to be placed off the O*O vector to satisfy hydronium's ideal pyramidal geometry (Fig. 5). When the acceptor's tilt angle is ~130°, an ideal pyramidal $\rm H_3O^+$ fits snugly in its place, but TIP3P's tilt angle is too large for that. Idealized H3 placement breaks the transfer H-bond 90% of the time in TIP3P, 22% in AIMD non-PT frames, 12% in AIMD PT frames, and 2% in TIP5P. This is the reason that $\Delta E_{\rm don-acc}$ is so large for TIP3P and improves substantially in TIP5P.

4. 1st shell interactions

We now turn to the analysis of the 1st shell contribution, which is related to H-bonding. First we consider H bond acceptance and then donation. Due to its charge, the hydronium is expected to be a poor acceptor of H-bonds. Indeed, as seen in Table III, it accepts an H-bond only 12% of the time in the non-PT AIMD frames, and either 19% or 0% in the classical systems. Formation of this H-bond is considered to initiate proton hop attempts.²³ Indeed, H-bond acceptance by $\rm H_3O^+$ increases to 29% in PT AIMD frames (Table III) and ΔE_{hop} is lower when this H-bond exists (Table IV).

The proton acceptor water molecule accepts one H-bond from the hydronium. It may also accept a second H-bond from another water molecule. In the AIMD trajectory, this happens 76% of the time. In fact, loss of this additional H-bond is thought to be the rate

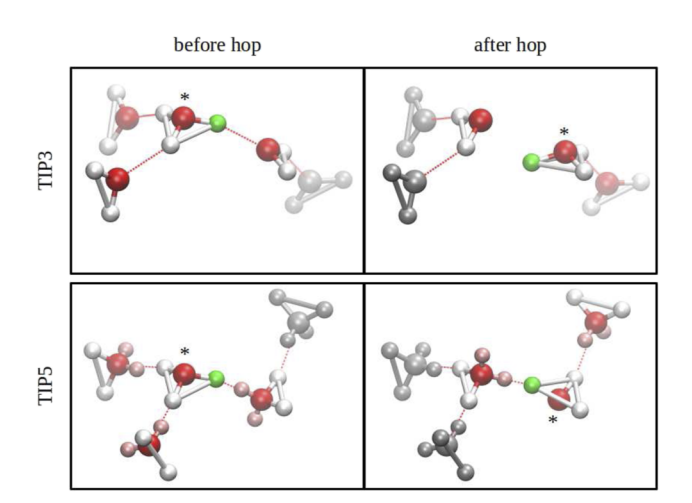


FIG. 5. Typical instant proton hops in the classical systems. H3O's O is marked with *. The hopping H3 is depicted in green. H-bonded molecules in the 2nd solvation shell are depicted in gray and H-bonds are depicted as red dashed lines.

TABLE III. Average number of H-bonds accepted by the H_3O^+ and the acceptor water molecule. This number is in addition to the transfer H-bond. After a hop, the numbers below will be swapped. The H-bond criterion is \geq 140° D-H···A H-bond angle and \leq 3.25 Å O···O distance. Error bars are standard deviations.

	By the H_3O^+	By the acceptor H_2O
AIMD (cov <1.15 Å)	0.12 ± 0.32	0.76 ± 0.48
AIMD (cov >1.15 Å) ^a	0.29 ± 0.45	0.45 ± 0.52
pH3O in TIP3	0.19 ± 0.39	0.07 ± 0.25
svH3O in TIP5	0.00 ± 0.06	0.34 ± 0.48

 $^{^{}m a}$ Only hops along the stretched covalent bond are included (~3000 frames), not hops to the other acceptors along bonds of normal length. Note that hopping frames include frames before and after a hopping event.

limiting step for proton transfer. 10,34,35 We find that indeed, the existence of this H-bond contributes unfavorably to ΔE_{hop} (Table IV). In the classical simulations, acceptance of an additional H-bond occurs less often, especially in TIP3P. In fact, $H_3\mathrm{O}^+$ accepts an additional H-bond more often than a TIP3P in the 1st solvation shell. The wrong tilt angle is partly responsible for this. TIP5P has the correct tilt angle, but still it accepts an additional H-bond about half

TABLE V. Average number of H-bonds donated by the H_3O^+ and the acceptor water molecule, before and after the hop. The criterion for $H_3O^+\cdots H_2O$ H-bonds is $\geq 140^\circ$ D-H···A H-bond angle and \leq either 2.90 Å (AIMD, TIP3P) or 2.70 Å (TIP5) O···O distance. For $H_2O\cdots H_2O$ H-bonds it is $\geq 140^\circ$ H-bond angle and ≤ 3.25 Å O···O distance. Error bars are standard deviations.

	By the H ₃ O ⁺		By the acceptor H ₂ O	
	Before	After	Before	After
AIMD (cov <1.15 Å) AIMD	2.97 ± 0.16	2.41 ± 0.70	1.91 ± 0.29	1.98 ± 0.13
(cov >1.15 Å) ^a pH3O in TIP3P svH3O in TIP5	2.95 ± 0.22	1.11 ± 0.25		1.95 ± 0.22

^aOnly hops along the stretched covalent bond are included (~3000 frames), not hops to the other acceptors along bonds of normal length. Note that hopping frames include frames before and after a hopping event.

as often as AIMD. Repulsion of water hydrogens by the ${\rm H_3O^+}$ may be responsible for this. If acceptance of an additional H-bond by the acceptor hinders PT, then one would expect PT to be favored in the classical systems. However, this is not observed.

Table V shows the number of H-bonds donated. In AIMD the hydronium donates close to 3 H bonds and the acceptor water close to 2, and this does not change significantly after a hop (when the hydronium and the acceptor are interchanged). In the classical systems the hydronium also donates 3 H-bonds and the acceptor water somewhat less than 2. But there is a large reduction in the number of H-bonds donated by the hydronium after the hop. For TIP3P the wrong tilt angle contributes about one H-bond to this problem. But the same problem also exists in TIP5P, where the transfer H-bond remains intact.

The reason for this can be found in the RDFs. The optimal $O \cdot \cdot \cdot O$ distance for two waters is about 2.8 Å (Fig. S3) and for H_3O^+ -water about 2.5–2.6 Å (Fig. 2). When the acceptor becomes hydronium its $O \cdot \cdot \cdot O$ distances from its H-bond accepting neighbors are too long for hydronium-water H-bonds. Conversely, the distances of the new water with its two other neighbors are too short for water-water H-bonds. These shifts make very large contributions to ΔE_{hop} . Figure 6 shows that the pair potential is sensitive to the distance near the minimum. A shift of 0.2 Å in hydronium-water distance costs about 5 kcal/mol. A similar shift in water-water distance costs about 2 kcal/mol. Thus, the total cost of the mismatch

TABLE IV. Contribution of an additional H-bond donated to the proton donor H_3O^+ or the acceptor H_2O (kcal/mol) to ΔE_{hop} Error bars are standard deviations.

	Donated to H ₃ O ⁺	Donated to H ₂ O		
Classical trajectories				
TIP3P pH3O	-2.10 ± 1.42	2.63 ± 4.09		
TIP5P svH3O	-3.19 ± 1.27	5.10 ± 1.60		
	AIMD trajectory evaluated with classical poten	itials (all cov < 1.15 Å)		
TIP3P pH3O	-1.09 ± 1.09	1.52 ± 2.17		
TIP5P svH3O	-4.27 ± 1.32	5.16 ± 1.91		

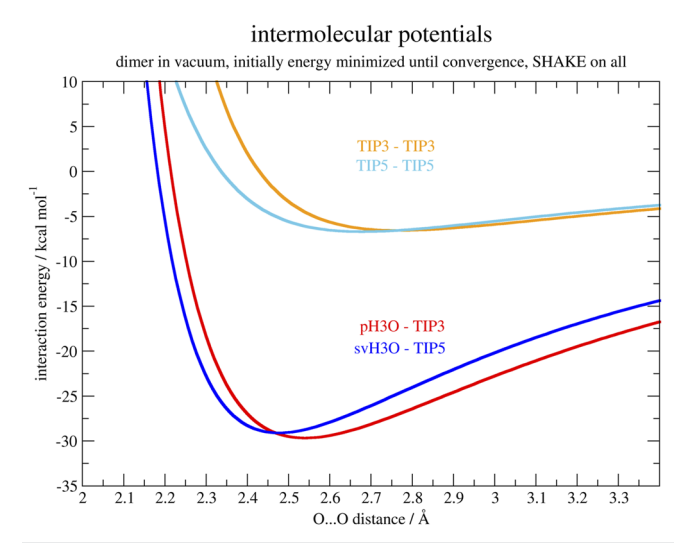


FIG. 6. Pair interactions in the gas phase between a H₃O⁺ and a water, or between two waters. The curves were calculated by first minimizing the energy of the pair and then increasing or decreasing their distance along the O··O axis.

may be up to 14 kcal/mol or even higher, if the water-water distances are longer than optimal, which seems to be true judging from the number of H-bonds donated in Table V. About a third of an acceptor TIP3P's donated H-bonds are too short and break upon instant PT. In TIP5P, the problem even increases to two thirds. This goes a long way toward explaining the $\Delta E_{don\text{-}1st}$ in Table II, which is about 30 kcal/mol and also includes a contribution from accepted H-bonds (Table IV).

IV. CONCLUSIONS

We have compared an ab initio simulation trajectory of an excess proton in water with classical trajectories of hydronium in TIP3P and TIP5P water. The classical trajectories showed large unfavorable potential energy changes (ΔE_{hop}) upon instantaneous proton transfer. The ab initio configurations were much more favorable, with a sizeable fraction giving a negative $\Delta E_{\rm hop}.$ This discrepancy was traced to geometric differences in the 1st and 2nd solvation shells. The classical simulations reproduce the ab initio position and number of H-bond acceptors within hydronium's 1st solvation shell but TIP3P's orientation (tilt angle) is off due to the lack of lone pairs, so the transfer H-bond breaks upon hopping. This can be alleviated with the use of TIP5P, where the transfer H-bond remains

Beyond tilt angle, the main feature that makes classical configurations less favorable to instant PT is the acceptor's donated H-bonds. H₃O⁺ is a strong H-bond donor. An acceptor water molecule in the 1st shell that is to become the next hydronium needs to donate two strong H-bonds into the 2nd shell. Ab initio water molecules are polarizable and that allows them to be better H-bond donors (Table V) even in non-transfer configurations. In the classical trajectories, the 2nd solvation shell is inaccurate. While shell structure is improved by the use of TIP5P, its lower partial charges lead to weak 1st shell-2nd shell H-bonds, which leads to a dramatic loss of donated H-bonds by the new H₃O⁺ after the hop. Since the intermolecular pair potential is steep around the minimum, even small displacements in this part of the new 1st solvation shell contribute strongly and unfavorably to ΔE_{hop} .

In past analyses of the proton transfer mechanism in water emphasis has been placed on the "fourth" accepted H-bond that is either formed by hydronium or breaks in the acceptor water. Both events facilitate the transfer because they make the solvation structure of hydronium more water-like and of the acceptor water more hydronium-like (the "presolvation" concept). This effect is also found here (Table IV) but contributes less to the energy gap than donated H-bonds, even in the ab initio configurations. Their contribution is even smaller in the classical configurations, where they are far outweighed by the mentioned mismatch in the donated H-bond lengths. The effect of donated H-bonds has not received much attention in the proton transfer literature as yet.

Can classical simulations of hydronium in water be improved to reproduce more closely ab initio trajectories? The 1st solvation shell (and the solvation free energy) is reproduced reasonably well by properly matching hydronium and water models, although the first peak of the RDF remains somewhat too high (Fig. 2). The 2nd solvation shell structure is harder to improve. Use of TIP5P could alleviate part of the problem. However, TIP5P is more expensive and its compatibility with biomolecular force fields has not been extensively tested. The special protonatable water molecules that the MOBHY algorithm places around the hydronium could perhaps be modeled after TIP5P with the bulk of the solvent remaining TIP3P. However, a discontinuity would arise when regular solvent molecules diffusing into the shell would have to be swapped out.

The H-Bond length mismatch could likely be alleviated by the use of polarizable classical models. Polarizability allows larger fluctuations that would lead to more frequent sampling of configurations stabilizing the PT product state. Such models are available for simple aqueous solution³⁶⁻⁴⁰ but extension to biological systems creates again issues of compatibility with standard biomolecular force fields. It might be possible, as above, to introduce polarizability only in the hydronium and the protonatable waters around it. Alternatively, the hopping protocol could be refined by moving accepting waters closer to the new hydronium. Preliminary calculations showed that this leads to lowering of ΔE_{hop} but not full recovery of the ab initio distribution.

Further improvements could be made in H3O's dynamics. Umbrella inversion, which should be a frequent event based on the low inversion barrier, 41,42 is observed once in the ab initio trajectory. This inversion is normally not allowed in classical hydronium models, especially when held rigid by SHAKE or similar constraints. AIMD studies showed that umbrella inversion affects proton transport. 43 In preliminary studies we have found that it is possible to get a reasonable inversion frequency in classical models by tuning the constraints and the force constants.

Despite the limitations, classical simulations with TIP3P could still offer insights into biological problems.⁴⁴ The deficiencies of TIP3P necessitate the use of a high threshold ΔE_{hop} for accepting proton hops, so as to reproduce the expected rate of proton movement (20 kcal/mol for svH3O and 23 kcal/mol for pH3O²¹). The relative effects of the environment (confinement, interaction

with charged and polar residues) are likely to be captured correctly by the classical force field. However, for higher accuracy in the configurations sampled, these deficiencies should be amended.

SUPPLEMENTARY MATERIAL

See the supplementary material for six figures with additional data.

ACKNOWLEDGMENTS

We thank Dr. Mark E. Tuckerman for providing the AIMD trajectory and Dr. Aliasghar Sepehri for help with the analysis. Funding was provided by the National Science Foundation (No. MCB-1855942).

AUTHOR DECLARATIONS

Conflict of Interest

The authors have no conflicts to disclose.

Author Contributions

MM performed all the analyses. MM and TL wrote the manuscript.

Manuela Maurer: Conceptualization (equal); Formal analysis (lead); Investigation (lead); Methodology (lead); Visualization (lead); Writing – original draft (lead); Writing – review & editing (equal). Themis Lazaridis: Conceptualization (equal); Funding acquisition (lead); Project administration (lead); Supervision (lead); Writing – review & editing (equal).

DATA AVAILABILITY

The data that supports the findings of this study are available within the article and its supplementary material.

REFERENCES

- 1 B. Winter, M. Faubel, I. V. Hertel, C. Pettenkofer, S. E. Bradforth, B. Jagoda-Cwiklik, L. Cwiklik, and P. Jungwirth, "Electron binding energies of hydrated ${\rm H_3O^+}$ and ${\rm OH^-}$: Photoelectron spectroscopy of aqueous acid and base solutions combined with electronic structure calculations," J. Am. Chem. Soc. **128**(12), 3864–3865 (2006).
- 2 W. Kulig and N. Agmon, "Both Zundel and Eigen isomers contribute to the IR spectrum of the gas-phase $\rm H_9O_4^+$ cluster," J. Phys. Chem. B 118(1), 278–286 (2014).
- 3 J. A. Fournier, W. B. Carpenter, N. H. C. Lewis, and A. Tokmakoff, "Broadband 2D IR spectroscopy reveals dominant asymmetric $H_{5}O_{2}^{+}$ proton hydration structures in acid solutions," Nat. Chem. 10(9), 932–937 (2018).
- ⁴O. Markovitch, H. Chen, S. Izvekov, F. Paesani, G. a. Voth, and N. Agmon, "Special pair dance and partner selection: Elementary steps in proton transport in liquid water," J. Phys. Chem. B 112(31), 9456–9466 (2008).
- ⁵P. B. Calio, C. Li, and G. A. Voth, "Resolving the structural debate for the hydrated excess proton in water," J. Am. Chem. Soc. **143**(44), 18672–18683 (2021). ⁶B. Hille, *Ionic Channels in Excitable Membranes*, 2nd ed. (Sinauer, 1991).

- 7 J. H. Wang, C. V. Robinson, and I. S. Edelman, "Self-diffusion and structure of liquid water. III. Measurement of the self-diffusion of liquid water with H^2 , H^3 and O^{18} as Tracers 1 ," J. Am. Chem. Soc. 75, 466–470 (1953).
- ⁸S. A. Fischer, B. I. Dunlap, and D. Gunlycke, "Correlated dynamics in aqueous proton diffusion," Chem. Sci. **9**(35), 7126–7132 (2018).
- ⁹S. Woutersen and H. J. Bakker, "Ultrafast vibrational and structural dynamics of the proton in liquid water," Phys. Rev. Lett. **96**(13), 138305 (2006).
- ¹⁰M. Tuckerman, K. Laasonen, M. Sprik, and M. Parrinello, "*Ab initio* molecular dynamics simulation of the solvation and transport of hydronium and hydroxyl ions in water," J. Chem. Phys. **103**(1), 150–161 (1995).
- ¹¹D. Marx, M. E. Tuckerman, J. Hutter, and M. Parrinello, "The nature of the hydrated excess proton in water," Nature **397**(6720), 601–604 (1999).
- ¹²D. Marx, A. Chandra, and M. E. Tuckerman, "Aqueous basic solutions: Hydroxide solvation, structural diffusion, and comparison to the hydrated proton," Chem. Rev. 110(4), 2174–2216 (2010).
- ¹³ M. Chen, L. Zheng, B. Santra, H. Y. Ko, R. A. DiStasio, Jr., M. L. Klein, R. Car, and X. Wu, "Hydroxide diffuses slower than hydronium in water because its solvated structure inhibits correlated proton transfer," Nat. Chem. 10(4), 413–419 (2018).
- 14 G. A. Voth, "Computer simulation of proton solvation and transport in aqueous and biomolecular systems," Acc. Chem. Res. **39**(2), 143–150 (2006).
- ¹⁵C. Knight and G. A. Voth, "The curious case of the hydrated proton," Acc. Chem. Res. 45(1), 101–109 (2012).
- ¹⁶M. A. Lill and V. Helms, "Molecular dynamics simulation of proton transport with quantum mechanically derived proton hopping rates (Q-HOP MD)," J. Chem. Phys. 115(17), 7993–8005 (2001).
- ¹⁷M. G. Wolf, H. Grubmuller, and G. Groenhof, "Anomalous surface diffusion of protons on lipid membranes," Biophys. J. **107**(1), 76–87 (2014).
- ¹⁸W. Zhang and A. C. T. Van Duin, "Second-generation ReaxFF water force field: Improvements in the description of water density and OH-anion diffusion," J. Phys. Chem. B 121(24), 6021–6032 (2017).
- ¹⁹ M. E. Selvan, D. J. Keffer, S. Cui, and S. J. Paddison, "A reactive molecular dynamics algorithm for proton transport in aqueous systems," J. Phys. Chem. C 114(27), 11965–11976 (2010).
- ²⁰L. Konermann and S. Kim, "Grotthuss molecular dynamics simulations for modeling proton hopping in electrosprayed water droplets," J. Chem. Theory Comput. 18(6), 3781–3794 (2022).
- ²¹T. Lazaridis and G. Hummer, "Classical molecular dynamics with mobile protons," J. Chem. Inf. Model. 57(11), 2833–2845 (2017).
- ²²B. R. Brooks, C. L. Brooks, 3rd, A. D. Mackerell, Jr., L. Nilsson, R. J. Petrella, B. Roux, Y. Won, G. Archontis, C. Bartels, S. Boresch *et al.*, "CHARMM: The biomolecular simulation program," J. Comput. Chem. 30(10), 1545–1614 (2009).
- ²³T. C. Berkelbach, H. S. Lee, and M. E. Tuckerman, "Concerted hydrogen-bond dynamics in the transport mechanism of the hydrated proton: A first-principles molecular dynamics study," Phys. Rev. Lett. **103**(23), 238302 (2009).
- ²⁴S. A. Fischer and D. Gunlycke, "Analysis of correlated dynamics in the Grotthuss mechanism of proton diffusion," J. Phys. Chem. B **123**(26), 5536–5544 (2019).
- ²⁵C. Arntsen, C. Chen, P. B. Calio, C. Li, and G. A. Voth, "The hopping mechanism of the hydrated excess proton and its contribution to proton diffusion in water," J. Chem. Phys. **154**, 194506 (2021).
- ²⁶ A. Hassanali, F. Giberti, J. Cuny, T. D. Kühne, and M. Parrinello, "Proton transfer through the water gossamer," Proc. Natl. Acad. Sci. U. S. A. 110(34), 13723–13728 (2013).
- ²⁷Y. L. S. Tse, C. Knight, and G. A. Voth, "An analysis of hydrated proton diffusion in *ab initio* molecular dynamics," J. Chem. Phys. **142**, 014104 (2015).
- ²⁸ R. Liu, C. Zhang, X. Liang, J. Liu, X. Wu, and M. Chen, "Structural and dynamic properties of solvated hydroxide and hydronium ions in water from *ab initio* modeling," J. Chem. Phys. **157**, 024503 (2022).

- ²⁹D. E. Sagnella and G. A. Voth, "Structure and dynamics of hydronium in the ion channel gramicidin A," Biophys. J. **70**, 2043–2051 (1996).
- ³⁰ M. W. Mahoney and W. L. Jorgensen, "A five-site model for liquid water and the reproduction of the density anomaly by rigid, nonpolarizable potential functions," J. Chem. Phys. **112**(20), 8910–8922 (2000).
- ³¹ A. V. Onufriev and S. Izadi, "Water models for biomolecular simulations," Wiley Interdiscip. Rev.: Comput. Mol. Sci. 8, e1347 (2018).
- ³²G. Lamoureux and B. Roux, "Absolute hydration free energy scale for alkali and halide ions established from simulations with a polarizable force field," J. Phys. Chem. B 110(7), 3308–3322 (2006).
- ³³ A. Grossfield, P. Ren, and J. W. Ponder, "Ion solvation thermodynamics from simulations with a polarizable force field," J. Am. Chem. Soc. **125**, 15671–15682 (2003).
- ³⁴N. Agmon, "The Grotthuss mechanism," Chem. Phys. Lett. **244**, 456–462 (1995).
- 35T. J. F. Day, U. W. Schmitt, and G. A. Voth, "The mechanism of hydrated proton transport in water," J. Am. Chem. Soc. 122(48), 12027–12028 (2000).
- ³⁶R. E. Kozack and P. C. Jordan, "Empirical models for the hydration of protons," J. Chem. Phys. **96**(4), 3131–3136 (1992).

- ³⁷S. Walbran and A. A. Kornyshev, "Proton transport in polarizable water," J. Chem. Phys. **114**(22), 10039–10048 (2001).
- ³⁸ L. X. Dang, "Solvation of the hydronium ion at the water liquid/vapor interface," J. Chem. Phys. **119**(12), 6351–6353 (2003).
- ³⁹R. Vácha, V. Buch, A. Milet, J. P. Devlin, and P. Jungwirth, "Autoionization at the surface of neat water: Is the top layer PH neutral, basic, or acidic?," Phys. Chem. Chem. Phys. **9**(34), 4736–4747 (2007).
- ⁴⁰J. S. Hub, M. G. Wolf, C. Caleman, P. J. Van Maaren, G. Groenhof, and D. Van Der Spoel, "Thermodynamics of hydronium and hydroxide surface solvation," Chem. Sci. 5(5), 1745–1749 (2014).
- 41 T. Rajamäki, A. Miani, and L. Halonen, "Six-dimensional *ab initio* potential energy surfaces for $\rm H_3O^+$ and NH $_3$: Approaching the subwave number accuracy for the inversion splittings," J. Chem. Phys. 118(24), 10929–10938 (2003).
- $^{\bf 42}$ S. Yu, B. J. Drouin, J. C. Pearson, and H. M. Pickett, "Terahertz spectroscopy and global analysis of $\rm H_3O^+,$ " Astrophys. J., Suppl. Ser. $\bf 180(1)$, 119–124 (2009).
- ⁴³A. A. Hassanali, F. Giberti, G. C. Sosso, and M. Parrinello, "The role of the umbrella inversion mode in proton diffusion," Chem. Phys. Lett. **599**, 133–138 (2014)
- ⁴⁴T. Lazaridis, "Molecular origins of asymmetric proton conduction in the influenza M2 channel," Biophys. J. **122**(1), 90–98 (2023).